ELSEVIER

Thermochimica Acta 318 (1998) 71–82

thermochimica acta

Structuring and texturing aluminum oxides

Hans Georg Wiedemann[a], Jörg Nerbel[b], Armin Reller[b,*]

[a] *Mettler Toledo GmbH, 8603 Schwerzenbach, Switzerland*
[b] *Institute of Inorganic and Applied Chemistry, University of Hamburg, 20146 Hamburg, Germany*

Received 15 July 1997

Abstract

The synthesis of alumina exhibiting different crystallinities, textures and morphologies is described. The tailoring of amorphous or nanocrystalline alumina forms is effected by the thermochemical decomposition of selected mono- and polynuclear molecular precursors, i.e. aluminum alkoxides. The role of mesostructured alumina is shortly discussed. The growth of alumina whiskers is characterized and the synthesis of single-crystalline alumina, i.e. industrial alumina, sapphire and ruby, is mentioned. The various processes and products are characterized by means of thermoanalytical and spectroscopic techniques, X-ray diffractometry and electron microscopy. © 1998 Elsevier Science B.V.

Keywords: Alumina; Aluminum alkoxide precursors; Alumina whiskers; Mesoscopic alumina; Thermoanalytical investigations

1. Introduction

With a total annual production of more than 6.5 million tons, the oxides, oxyhydroxides and hydroxides of the elements aluminum, silicon and titanium are undoubtly among the most important industrial inorganic chemicals. Apart from aluminum metal with an estimated global production of 20 million tons per year, the aluminum oxides, oxyhydroxides and hydroxides are the second most important refined products of the natural mineral bauxite, of which 114 million tons were mined in 1995 [1]. Whereas titanium oxide is the most important white pigment, silica and the aluminum species are predominantly used as catalysts, catalyst supports, adsorbents, abrasive or hard materials, sapphire, ruby, and ceramic materials. This spectrum of applications requires a tailoring of intrinsic properties, such as particle size, particle morphology, surface, etc. Among the three mentioned metals, aluminum offers the richest variety of Al–O and Al–O–H phases [2]. The controlled synthesis of one or other phase therefore demands not only an appropriate choice of precursor systems, but also the reproducibility of synthesis parameters. In this report, we concentrate on synthesis pathways and the characterization of extremely different alumina products, i.e. microcrystalline alumina from selected novel precursors, alumina whiskers from selective oxidation of aluminum alloys, or large alumina crystals from different melting procedures. In addition, the preparations of mesophasic and single-crystalline alumina are briefly mentioned. Combined thermoanalytical methods, as well as comparative structural and morphological studies, allow detailed insights into the different mechanisms of product formation.

*Corresponding author. Tel: +49 40 41233103; fax: +49 40 41236348; email: reller@x-ray.chemie.uni-hamburg.de

PII S0040-6031(98)00331-1

2. Structuring and texturing nano- and microcrystalline alumina by using aluminum alkoxides and aluminum acetylacetonates as precursor systems

The preparation of nano- and microcrystalline functional alumina may be achieved by different methods (see e.g. [3,4]). To develop a low-temperature route, within which the morphology and the surface properties of the products may eventually be controlled, we set out to prepare mono-, di-, tri- and tetranuclear aluminum alkoxide and acetylacetonate (acac) precursors [6]. The idea was to hydrolyse these precursors to form a gel. The chemical transformations can be schematically described as:

$$\mathrm{Al(OR)_3} \rightarrow \mathrm{Al(OH)(OR)_2} \rightarrow \mathrm{Al(OH)_2(OR)} \rightarrow \mathrm{Al(OH)_3} \quad (1)$$

As the second step this gel is dried and thermally treated to transform it into the desired products. The parent alkoxide precursors can be prepared by different routes. In the first step, aluminum alkyls are reacted with alcohols according to the following general equation:

$$\mathrm{AlR_3} + 3\mathrm{R'OH} \rightarrow \mathrm{Al(OR')_3} + 3\mathrm{RH}\ (\mathrm{R}, \mathrm{R'} = \text{different alkyl groups}) \quad (2)$$

The volatile alkanes can then be completely removed or – in order to quantify the reaction – measured volumetrically. A disadvantage is the formation of usually pyrophoric aluminum alkyls. An alternative and more elegant way is the use of partially hydrolysed aluminoxanes. For example, one can start with a non-pyrophoric mixture of methylaluminoxane (MAO) [5] and partially hydrolysed methylaluminoxane. This mixture can be reacted with alcohols according to the following equation:

$$\mathrm{MAO} + 3\mathrm{R'OH} \rightarrow \mathrm{Al(OR')_3} + 3\mathrm{CH_4} \quad (3)$$

Analogous reactions can be performed using different acetylacetone species.

In the alkoxides, as well as in the acetylacetonates, the first-coordination sphere of the aluminum cation is made up of oxygen. This is the desired moiety for building up alumina by either the mentioned hydrolysis or by thermal degradation. To study the influence of the selected precursor on the product formation, the mononuclear aluminum-tris-1,1,1,6,6,6-hexamethylacetylacetonate (Fig. 1(a)), the dinuclear aluminum-*tert*-butanolate $Al_2(OC_4H_9)_6$ (Fig. 1(b)), the trinuclear aluminum-neo-pentanolate $Al_3(OC_5H_{11})_9$ (Fig. 1(c)) and the tetranuclear aluminum-tris-trimethylsilylmethanolate $Al_4[(OCH_2Si(CH_3)_3]_{12}$ (Fig. 1(d)) have been prepared as single crystals and their structure has been determined by X-ray diffraction [6].

The thermal decompositions of these precursor species have been investigated by means of combined thermal analysis and mass spectrometry. In Fig. 2 the thermal degradation of a dinuclear precursor, i.e. aluminum-*tert*-butanolate $Al_2(OC_4H_9)_6$, is shown. As can be seen, the degradation is completed slightly above 250°C, which is a comparatively low temperature. X-ray diffractometry reveals that the alumina product formed is amorphous, i.e. the formation of crystalline alumina domains is hampered by the low decomposition temperature, and also by the relatively large groups in the alkoxide precursor. This means that, during the thermal decomposition, a large decrease in the volume takes place. This effect also hinders the formation of crystalline product domains, because the reaction temperature does not allow a high mobility of the alumina fragments. As a consequence, alumina products obtained by this method exhibit large surfaces. As is observed by scanning electron microscopy, highly porous morphologies are obtained (Fig. 3(c)). The pore size and the crystallinity of the products can be influenced by the selection of the precursor species. As the high-resolution electron micrograph (Fig. 4) reveals, the highly crystalline domains of the alumina products have diameters of below 10 nm. In addition they do not exhibit a regular morphology, which can be quite attractive for different applications.

3. Mesophasic and mesoporous alumina

The controlled synthesis of mesophasic or mesoporous alumina is of considerable importance. Such products are supposed to be optimal catalysts or catalyst support materials with extremely high outer and inner surfaces, i.e. as molecular sieves. Early studies by Bagshaw and Pinnavaia [7] showed that, in analogy and extension to the molecular sieves of the M41S-type, mesoporous alumina can be synthesised

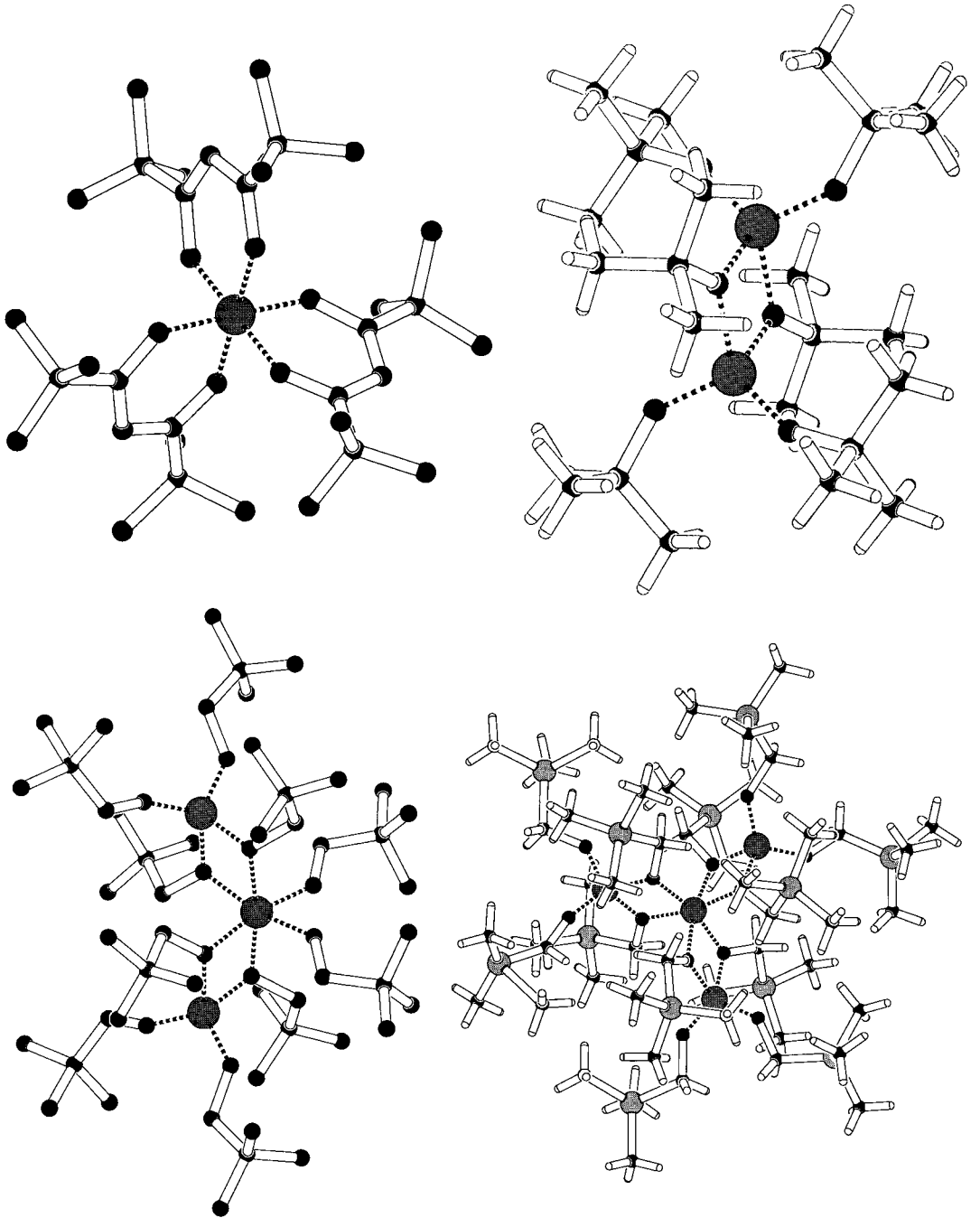

Fig. 1. Crystal structures of mono-, di-, tri- and tetranuclear precursors for the preparation of alumina exhibiting tailored morphologies and textures (small open spheres: hydrogen; small black spheres: carbon; small dotted spheres: oxygen; large dark dotted spheres: aluminum; in Fig. 1(d): bright dotted spheres: silicon). (a) Crystal structure of mononuclear aluminum-tris-1,1,1,6,6,6-hexamethylacetylaceonate with the aluminum ion in an octahedral oxygen moiety. (b) Crystal structure of dinuclear aluminum-*tert*-butanolate $Al_2(OC_4H_9)_6$ with the aluminum ions in tetrahedral oxygen moieties. (c) Crystal structure of trinuclear aluminum-neo-pentanolate $Al_3(OC_5H_{11})_9$ with one aluminum ion in a distorted octahedral and two aluminum ions in tetrahedral oxygen moieties. (d) Crystal structure of tetranuclear aluminum-tris-trimethylsilylmethanolate $Al_4[(OCH_2Si(CH_3)_3]_{12}$ with one aluminum ion in a distorted octahedral and three aluminum ions in tetrahedral oxygen moieties.

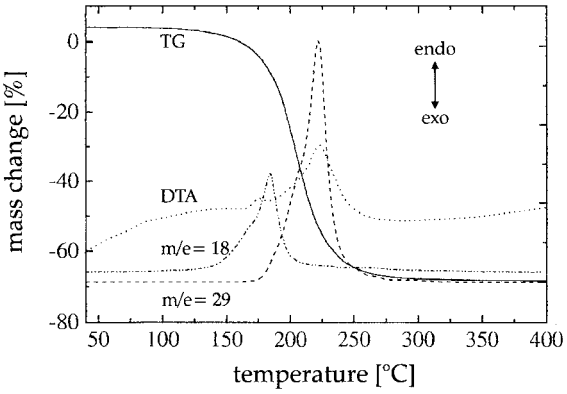

Fig. 2. Thermogravimetric and mass-spectrometric measurements of the decomposition of the partially hydrolysed dinuclear precursor aluminum-*tert*-butanolate $Al_2(OC_4H_9)_6$ in synthetic air (heating rate: 10°/min; 50 ml O_2/min). The masses registered by mass spectrometry are: *m/e*=18: water; *m/e*=29: C_2H_5-fragment of the *tert*-butanolate groups. The mass peak of CO_2, *m/e*=44, is not depicted; its high intensity is registered in the range from 170 to 260°C.

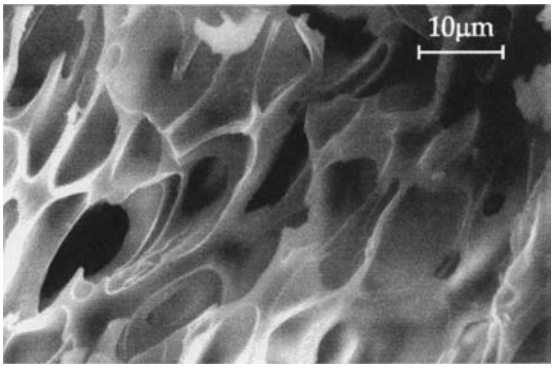

Fig. 3. Scanning electron micrograph of the highly porous alumina obtained from the thermal decomposition of the partially hydrolysed dinuclear precursor aluminum-*tert*-butanolate $Al_2(OC_4H_9)_6$.

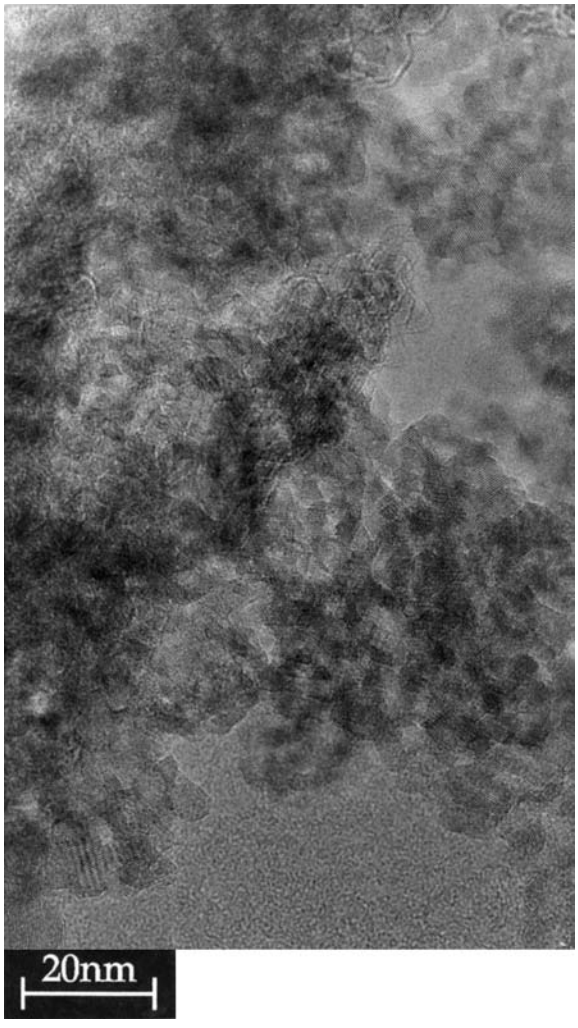

Fig. 4. High-resolution transmission electron micrograph of the alumina obtained from the thermal decomposition of the dinuclear precursor aluminum-*tert*-butanolate $Al_2(OC_4H_9)_6$. The size and shape of the nanoscopic, but highly crystalline alumina domains are clearly visible.

by hydrolysing tri-*sec*-butoxyaluminum in non-ionic polyethyleneoxide tensides and calcining the hydrolysis product at 773 K. The mesoporous alumina obtained had surface areas in the range from 420 to 530 m^2/g. A more recent paper by Yada et al. [8] reports on the synthesis of alumina-based mesophases templated by dodecyl sulfate and alkyl alcohols. The control of the surface morphologies and patterns of the surfactant assemblies is stated to be a promising modification technique for tailoring differently formed alumina products, and also for better understanding biomimetic patterning. One decisive factor guaranteeing the success of this approach is the mechanism of the thermochemical degradation of the surfactant assembly, i.e. the removal of the organic templates and, in the case of dodecyl sulfate and related compounds, also the removal of anionic species, i.e. their thermal-decomposition products. In many cases, the thermochemically induced removal of the template species leads to a collapse of the

mesostructure and nanocrystalline alumina is formed as the stable product. Alternative ways, such as extraction procedures or controlled hydrolyses, may allow the conservation of the mesostructure, as has been extensively performed for the synthesis of mesoporous silica, or alumophosphates, and also for the more complex alumosilicates and titanosilicates, which are thought to be very interesting catalysts or catalyst supports [9]. Knowledge of the chemistry of mesoporous products is still rudimentary, but the prospect of achieving many interesting structural and morphological modifications and attractive applications gives much interest to this research topic. The links to the nanosciences and biomimetics, as well as biomineralisation, are additional driving forces for a better understanding of these fascinating spatial frameworks of – in terms of chemical composition – rather simple compounds.

4. Growth of alumina whiskers

Alumina whiskers are nearly perfect, fibrous single crystals. Mineralogists have observed and described the phenomenon of whisker formation for centuries. They have been synthesized under many different conditions. The controlled production of specific whisker morphologies, however, is of crucial interest in view of practical applications. The first experiments demonstrating the 10- to 20-fold strengthening of various materials with corundum whiskers were performed many years ago [10]. The growth of alumina whiskers by vapour phase processes has been described by several researchers [11–16]. At present, the development and the quality of mono- or polyfunctional composite materials is being implemented in many different systems and processes demand reproducible and quantitative synthesis conditions. The conditions also have to guarantee the production of whiskers exhibiting specific shapes and sizes, crystallographic orientations of the growth axis, purity and mechanical properties. With regard to the known growth method, these parameters may be more or less well controlled. In this report, we focus on the modifications of the following synthesis routes:

1. thermal reduction of alumina with humid hydrogen (partial pressure of H_2O in the range of 10 mbar) or with carbon at temperatures above 1800°C;
2. thermal oxidation of aluminum in humid hydrogen (partial pressure of H_2O in the 10–100 mbar range) at temperatures between 1250 and 1600°C;
3. oxidation of aluminum in dry hydrogen in the presence of the co-reagents mullite or other silicate-type refractories; and
4. hydrolysis of $AlCl_3$ in a H_2/CO atmosphere above 1000°C.

The mechanisms of whisker formation depend on the methods mentioned: Aluminum suboxides, in particular Al_2O, are the species responsible for mass transport in the vapour phase (see e.g. [17,18]). Reactions between aluminum vapour and volatile silicon monoxide are thought to be the decisive steps for whisker growth according to the third method. These products usually contain more impurities than the ones obtained by the methods 1, 2 and 4. The exact control of the temperature conditions and the partial pressures of the oxidizing agents are decisive for the control of steady growth of one or other form of alumina whiskers. As has been described in the literature, the different growth mechanisms lead to the formation of so-called *A-type whiskers*, with the growth directions [1010] and [1120], and the *C-type whiskers* with the growth direction [0001]. As will be described below, mixtures of both growth directions are also observed (see also [19]).

To achieve detailed insights into the different temperature-dependent growth mechanisms and, therefore, to define synthesis conditions for the growth of one or other type of whisker, extensive thermoanalytical and morphological studies have been carried out. In Fig. 5, TG and DTA measurements of pure alumina are shown. The curves reveal the melting, slow evaporation and freezing or crystallizing characteristics in a oxygen atmosphere. For the growth of alumina whiskers the iron–aluminum alloy Fe_3Al was selected as an aluminum source [20]. This alloy was placed in an alumina crucible, which was covered with an alumina lid (Fig. 6). In a thermobalance (METTLER TA1), the formation of whiskers was followed quantitatively in the $1100 \leq T_{syn} \leq 1550$°C range. In Fig. 7 the products obtained, i.e. intergrown A-type and C-type whiskers, are shown as grown in the crucible. The reactions leading to the formation of

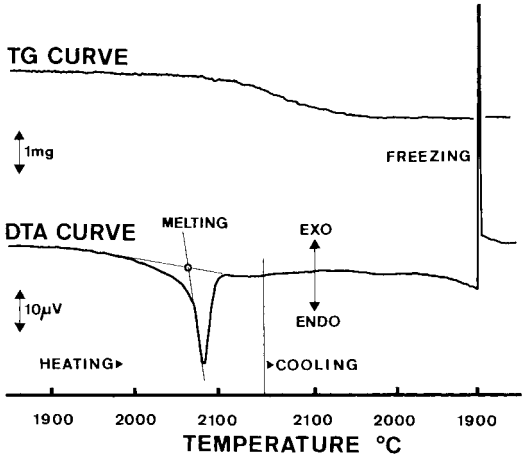

Fig. 5. TG/DTA measurements of the thermal behaviour, i.e. melting, evaporation and crystallization, of alumina in a vacuum (1.33×10^{-3} Pa). Sample weight: 40 mg; heating rate: 10°C min^{-1}; tungsten crucible.

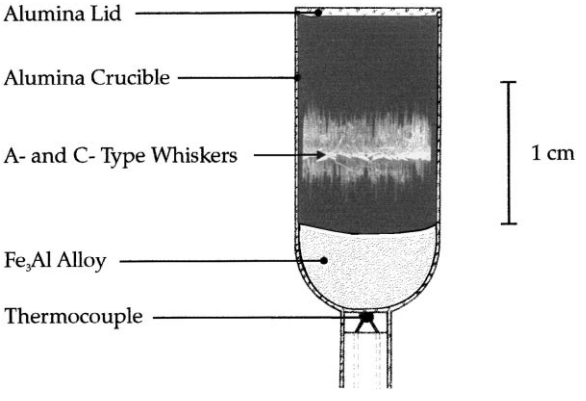

Fig. 6. Schematic view of the alumina crucible containing the starting material, Fe_3Al, as well as the whiskers formed.

these whiskers are as follows:

$$2Al_{(liquid)} + H_2O_{(gas)} \rightarrow Al_2O_{(gas)} + H_{2_{(gas)}} \quad (4)$$

$$Al_2O_{(gas)} + 2H_2O_{(gas)} \rightarrow Al_2O_{3_{(solid)}} + 2H_{2_{(gas)}} \quad (5)$$

Reactions (4) and (5) describe the transport processes. Overall reaction (6) describes the formation of A-type and C-type whiskers:

$$2Al_{(liquid)} + 3H_2O_{(gas)} \rightarrow Al_2O_{3_{(solid)}} + 3H_{2_{(gas)}} \quad (6)$$

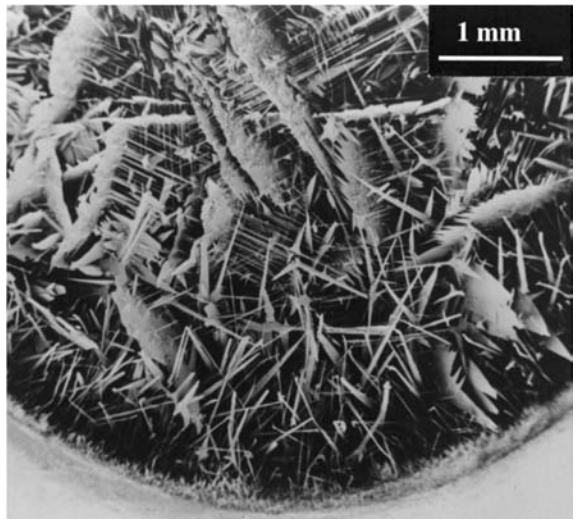

Fig. 7. Optical micrograph of the A-type and C-type whiskers as obtained in the alumina crucible by the reaction of the starting material, Fe_3Al, with water vapour.

Above 1800°C the following process is observed:

$$Al_2O_{3_{(solid)}} + 2H_{2_{(gas)}} \rightarrow Al_2O_{(gas)} + 2H_2O_{(gas)} \quad (7)$$

For the growth of whiskers, it is important to work with a sufficient partial pressure of H_2O. Apart from the partial pressure of H_2O, the concentration of the volatile aluminum suboxide and the temperature are the decisive parameters. Consequently, an important factor is whether the whiskers are grown in an open or in a closed crucible. In an open crucible many small whiskers are formed, whereas in closed crucibles slow growth rates lead to the formation of few, but comparatively large whiskers.

A series of experiments at various temperatures has been carried out to reveal the interdependence of reaction temperature, growth speed and growth mechanism, i.e. the type of whiskers formed under the given experimental conditions (see also [16]). In Fig. 8, the correlation between the growth rate of whiskers and the temperature in the 1200–1550°C range is presented. At comparatively low temperatures, i.e. ca. 1250°C, probably A-type whisker-like crystals grow from the inner surface of the crucible (see Fig. 9). At even lower temperatures the formation of hair-like, fibrous alumina crystals can be observed.

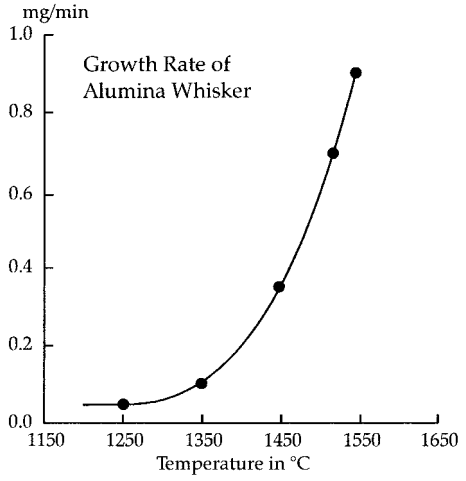

Fig. 8. A plot of whisker growth rate against temperature. Syntheses were performed at the temperatures indicated by the black dots on the graph.

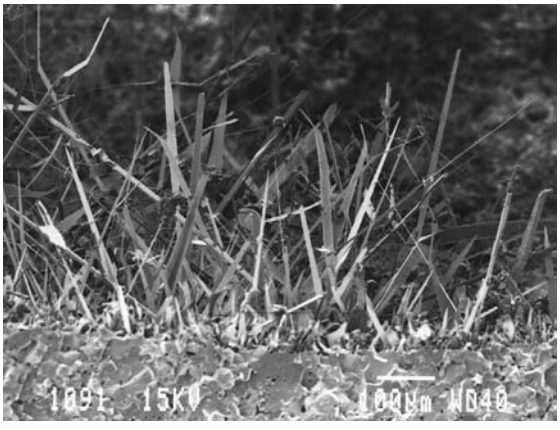

Fig. 9. A-type whiskers grown from the wall of the alumina crucible (visible at the bottom of the micrograph) at temperatures ca. 1250°C. Their morphology may be described as extremely thin ribbon-shaped needles.

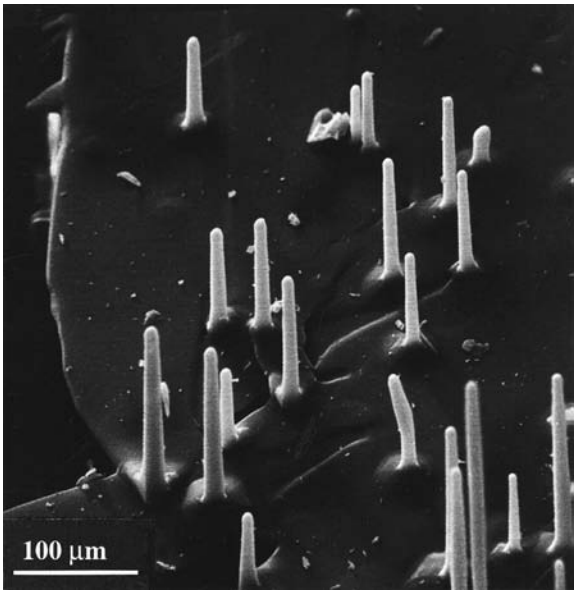

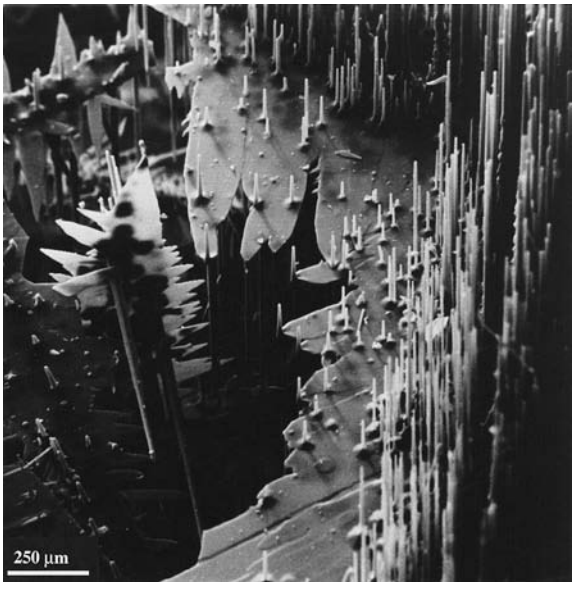

Fig. 10. Formation of C-type whiskers on the basal plane of A-type whiskers. (a) Very small, non-facetted needles of C-type whiskers. (b) Non-facetted C-type whiskers of different lengths on an A-type whisker platelet.

These two products cannot be described as crystallographically well-defined forms of whiskers.

Above 1250°C, the growth of extended thin plates of A-type whiskers is observed (see e.g. Fig. 7, Fig. 10, Fig. 11). As mentioned above, A-type whiskers are formed by preferential crystal growth perpendicular to the c-axis or along the crystallographic directions parallel to the (0001) plane, i.e. along the [1010] and/or [1120] directions. Thin plates up to few millimetres in diameter are obtained as products. It has been argued that this type of whisker growth is energetically favoured by the closer packing of the ions in the (0001) plane (see e.g. [15]).

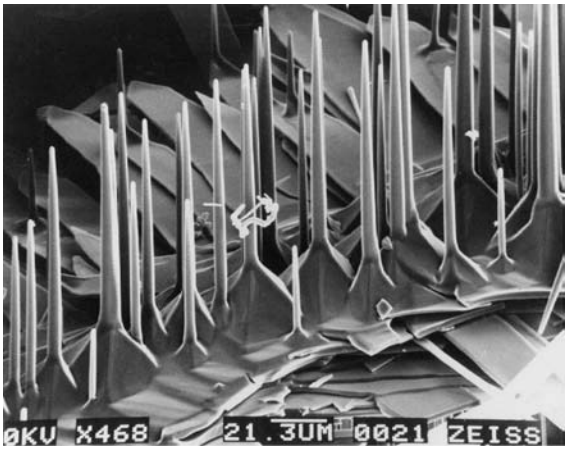

Fig. 11. Non-facetted C-type whiskers grown on facetted hexagonal capped pyramids. These pyramidal 'interfaces' form on the basal plane of A-type whiskers.

If the synthesis temperature is raised above 1500°C, one observes the formation of small, needle-shaped crystallites. They start growing on the basal planes (0001) of the A-type whiskers and their growth direction is perpendicular to these planes, i.e. along [0001]. As is shown in Fig. 10, the crystallites exhibit a cylindrical habit and their base, i.e. the 'interface' between the basal plane of the A-type whisker and the C-type whisker needle, is not yet facetted. However, electron diffraction confirms that the growth direction of these C-type whiskers is [0001]. At slightly higher temperatures the facetting of the base, as well as of the C-whiskers, becomes visible (Fig. 11). Fig. 12(a) confirms that the mentioned interface between plate-like A- and well-facetted, comparatively thick hexagonal C-type whiskers grows out of well-developed capped hexagonal pyramids. In many experiments platelets of A-type-whiskers, 'overgrown' by C-type whiskers, were obtained (Fig. 12(b)). Detailed studies on the mechanism of growth of C-type whiskers reveal that, at the beginning, hexagonal, capped pyramids form on the basal planes of the A-type whisker (Fig. 12(c)). In many cases a condensation droplet is seen on the pyramid and – in a further stage – C-type whiskers grow. This droplet-like growth nucleus, formed by vapour phase mass transport, i.e. vapour condensation, can also be observed on the tips of grown whiskers. Depending on the experimental conditions, the hexagonal facetting of the whiskers is more or less perfect (Fig. 12(d)). Temperature fluctuations may influence the steady growth along the c-direction leading to imperfect crystals, i.e. A-type whisker growth competes with C-type whisker growth (Fig. 13(a) and Fig. 13(b)). It is even possible to attain experimental conditions where step-wise spiral growth of A-type whiskers along [0001] leads to hexagonally arranged petal-like agglomerates (Fig. 13(c)). Large natural corundum crystals, which exhibit a hexagonal-bipyramidal habit may have been formed by a related growth mechanism (Fig. 14).

5. Large alumina single crystals

Owing to their clarity, brilliance, hardness, refractive index and chemical inertness, pure and doped large alumina single crystals find many technical applications [2]. Here, we only focus on the industrial high-temperature crystal growth, which plays a crucial role in the production of alumina phases exhibiting specific optical and mechanical properties. At present, the method first developed by A.V.L. Verneuil is used for the generation of synthetic corundum, white, yellow and blue sapphire as well as ruby crystals [21,22]. These phases are grown in furnaces heated with a carbon-free hydrogen/oxygen flame at temperatures well above 2000°C (melting point of alumina: ~2050°C) and it is nowadays possible to produce crystals of more than 3000 carats. In Fig. 15, an in-situ view of a working furnace with a growing sapphire crystal is shown. A collection of sapphire and ruby crystals in different growth stages is presented in Fig. 16. Such crystals are cut and extensively used in the watch industry, for jewellery, for mechanical applications, etc. A very important extension of the spectrum of properties of alumina single crystals is achieved by doping. By precipitation of titania in the alumina matrix, special optical effects like the so-called asterism, i.e. the six-branched star, are achieved. Moreover, the doping of alumina with selected transition-metal cations allows the synthesis of lasers and masers [23]. Using very small amounts of Ti^{3+} dopant (content <0.15%) allows the production of tunable lasers operating between 700 and 1050 nm [24]. Such single-crystalline materials are obtained either by the Verneuil method, or by the Czochralski method, or by the heat-exchanger method [22].

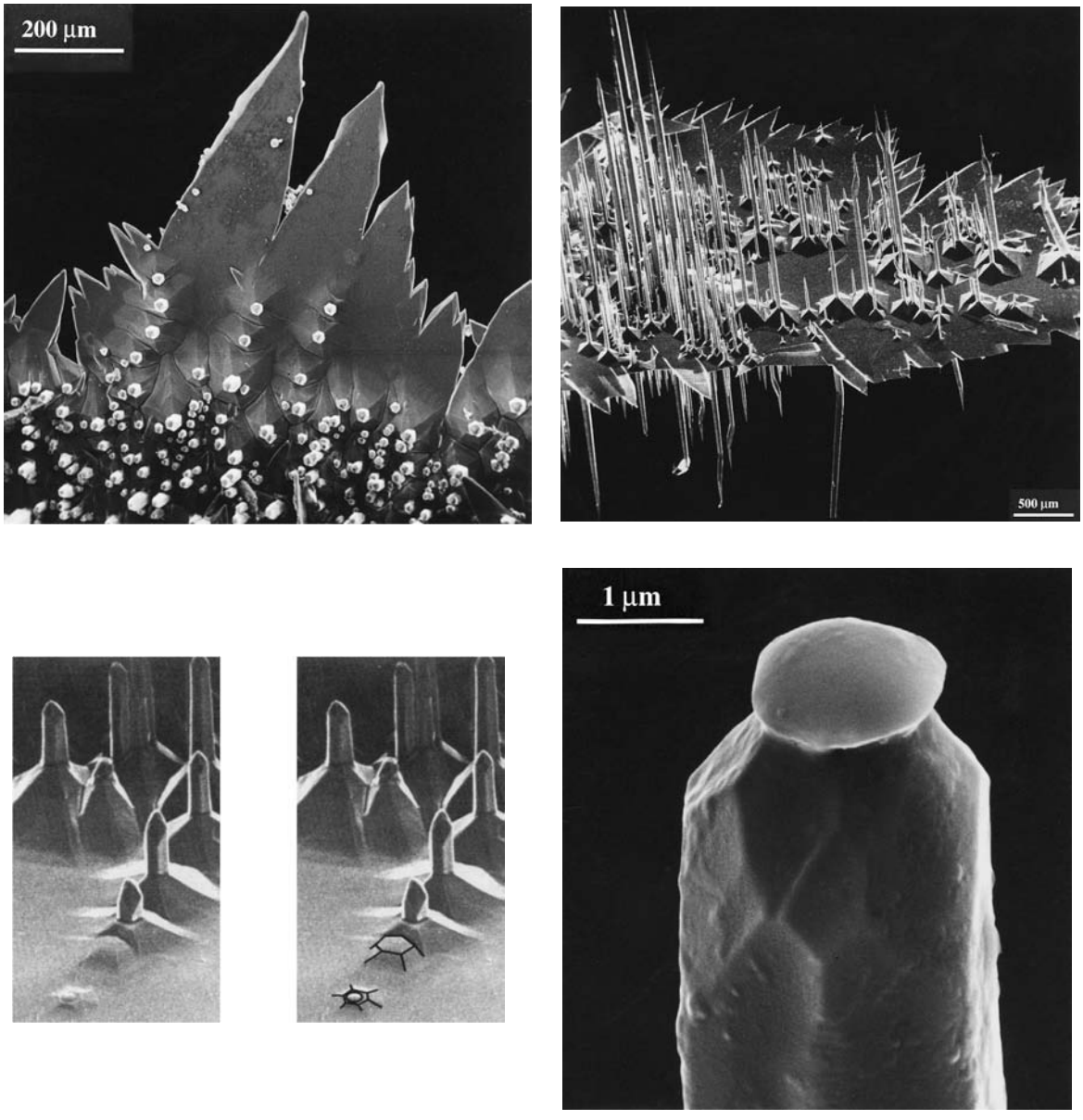

Fig. 12. Formation of well-facetted C-type whisker nuclei on well-facetted capped hexagonal pyramids. These pyramidal interfaces are located on the basal plane of A-type whisker platelets. (a) Nucleation of well-facetted C-type whiskers on well-facetted capped hexagonal pyramids. (b) An A-type whisker platelet 'overgrown' with well-facetted C-type whiskers. (c) Detail of the nucleation phase of C-type whiskers. The formation of a capped hexagonal pyramid, the condensation droplet and well facetted, small C-type whiskers with a diameter of ca. 1 μm are visible. In order to visualize the facetting of the capped hexagonal pyramid, the edges have been drawn. (d) Condensation droplet on the tip of a C-type whisker, which is in the stage of developing facets.

6. Conclusions and perspectives

The future of aluminum oxides in various forms is obviously very bright. Whether in single-crystalline form, or as a powder with very high surface areas, or as a fibrous component of composite materials, this metal oxide proves to be one of the most economic, least toxic or environmentally harmful, as well as highly

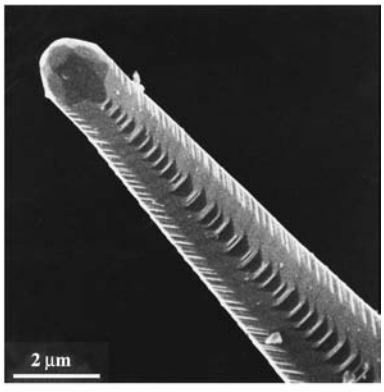

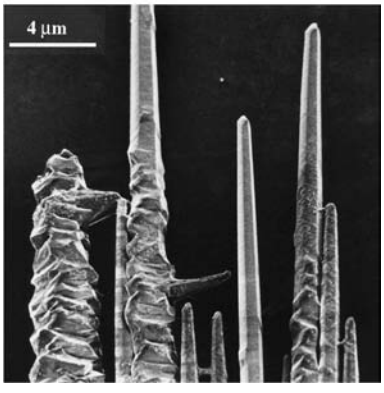

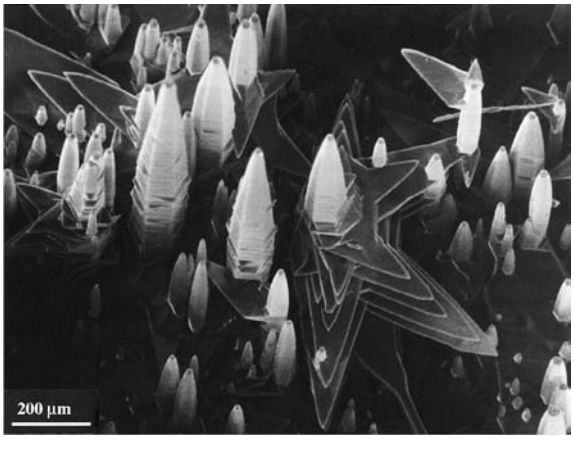

Fig. 13. Temperature fluctuations lead to imperfect C-type whiskers (a) and (b) [15], or to (c) hexagonally agglomerated A-type whisker platelets joined along the crystallographic direction [0001].

Fig. 14. Natural corundum crystals exhibiting a hexagonal-bipyramidal habit (samples found in Sri Lanka).

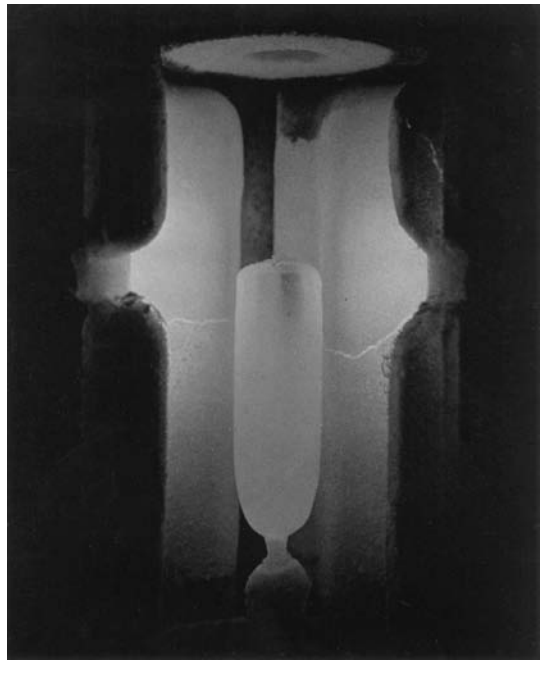

Fig. 15. View into a furnace, wherein a corundum crystal is grown by the verneuil method. Length of the crystal: ca. 12 cm (photograph by courtesy of DJÉVAHIRDJIAN SA, CH-Monthey).

economic, industrial metal oxides. As we have tried to show, the controlled generation of one or other aluminum oxide product exhibiting specific morphological and/or textural features requires accurate measurements of the thermochemical properties of the parent and product materials and also reproducible and reliable thermodynamic data for the production engineering, as well as for safe implementation in

Fig. 16. Collection of ruby and sapphire crystals at different growth stages obtained by the verneuil method. Length of the longest crystal: ca. 12 cm (photograph by courtesy of DJÉVA-HIRDJIAN SA, CH-Monthey).

technical and industrial applications. Combined thermoanalytical techniques proved to be versatile and highly informative tools for achieving detailed insights into the structure/property/reactivity features of aluminum oxides and thus form the basis for successful research, development and production activities.

Where are the new frontiers and forthcoming developments in the chemistry and physics of aluminum oxides? There is no doubt that novel, partly volatile precursor systems will open the way to the production of thin films exhibiting useful surface or mechanical properties (see e.g. [25]). The knowledge and experience achieved by research on alumina precursors has been transferred to the synthesis of heterometallic molecular, partly soluble precursors for the low-temperature synthesis of aluminosilicates (see e.g. [26]), aluminophosphates or silicoaluminophosphate phases, together with templates also for mesoporous products. These materials are thought to be most active, and also shape selective, as acid/base catalysts. Finally, the demands for high-tech ceramics and gradient materials will enhance dedicated studies of the phenomenology and the tailoring of aluminum oxides or their appropriate precursors. The accurate characterization of the atomic and electronic structures, of the morphology, the texture and habit and, in particular, the study of reaction mechanisms and kinetics leading from selected parent phases to the desired products will also continue to depend in future on reliable results obtained from combined thermal analysis, diffractometry, spectroscopy and, last but not least, the intuition and experience of researchers and engineers.

Acknowledgements

The authors are grateful to R. Wessicken for electron microscopic investigations, to U. Sazama for graphs and illustrations and to the Bundesamt für Energie (Bern, Switzerland) as well as the Fonds der Chemischen Industrie (Frankfurt, Germany) for financial support.

References

[1] Der Fischer Weltalmanach, Fischer Taschenbuch Verlag, Frankfurt, 1998.
[2] A. Petzold, J. Ulbricht, Aluminiumoxid: Rohstoff, Werkstoff, Werkstoffkomponente, Deutscher Verlag für Grundstoffindustrie, Leipzig, 1991.
[3] D.C. Bradley, R.C. Mehrotra, D.P. Gaur, Metal Alkoxides, Academic Press, London, 1978.
[4] C.J. Harlan, M.R. Mason, A.R. Barron, Organometallics 13 (1994) 2957.
[5] K.A. Andrianov, A.A. Zhadanov, J. Polym. Sci. 30 (1958) 513.
[6] J. Nerbel, Ph.D. Thesis, University of Hamburg, 1997.
[7] S.A. Bagshaw, T.J. Pinnavaia, Angew. Chem. 108 (1996) 1180.
[8] M. Yada, H. Kitamura, M. Machida, T. Kijima, Langmuir 13 (1997) 5252.
[9] A. Corma, Chem. Rev. 97 (1997) 2373.
[10] Sci. Newsletter, 81(1) (1962) 11.
[11] W.W. Webb, W.D. Forgang, J. Appl. Phys. 28 (1957) 1449.
[12] R.C. DeVries, G.W. Sears, J. Chem. Phys. 31 (1959) 1256.
[13] G.W. Sears, R.C. DeVries, J. Chem. Phys. 39 (1963) 2837.
[14] W.B. Campbell, Chem. Eng. Progr. 62 (1966) 68.
[15] H.G. Wiedemann, E. Sturzenegger, G. Bayer, R. Wessicken, Naturwissenschaften 61 (1974) 65.
[16] H.G. Wiedemann, G. Bayer, Trends and Applications of Thermogravimetry, Topics in Current Chemistry, Springer Verlag, Berlin, Heidelberg, New York, 1978, p. 121 ff.
[17] J. Drowart, G. DeMaria, R.P. Burns, M.G. Ingraham, J. Chem. Phys. 32 (1959) 1366.
[18] R.C. Paule, High Temp. Sci. 8 (1976) 257.
[19] T. Hayashi, M. Iwata, H. Saito, Bull. Chem. Soc. Jpn. 56 (1983) 1235.

[20] H. Kleykamp, H. Glasbrenner, Z. Metallkd. 88 (1997) 230.
[21] K. Nassau, J. of Crystal Growth 13/14 (1972) 12.
[22] Hrand DJEVAHIRDJIAN S.A., Industrie de Pierres Scientifiques, Monthey, Switzerland, private communication.
[23] A. Kistler, Rev. Hautes Tempér. et Réract. 2 (1965) 25.
[24] R. Moncorgé, G. Boulon, D. Vivien, A.M. Lejus, R. Collongues, V. Djévahirdjian, K. Djévahirdjian, R. Cagnard, IEEE J. of Quantum Electronics 24 (1988) 1049.
[25] W.A. Herrmann, N.W. Huber, O. Runte, Angew. Chem. 107 (1995) 2371.
[26] M.L. Montero, I. Usón, H.W. Roesky, Angew. Chem. 106 (1994) 2199.